Journal of Catalysis 279 (2011) 310–318

Contents lists available at ScienceDirect

Journal of Catalysis

journal homepage: www.elsevier.com/locate/jcat

Novel approach to rhenium oxide catalysts for selective oxidation of methanol to DMM

Olesya A. Nikonova [a,*], Mickaël Capron [b,c], Ge Fang [b,c], Jérémy Faye [b,c], Anne-Sophie Mamede [b,c,d], Louise Jalowiecki-Duhamel [b,c], Franck Dumeignil [b,c,e], Gulaim A. Seisenbaeva [a]

[a] Department of Chemistry, SLU, Box 7015, SE-75007 Uppsala, Sweden
[b] Univ. Lille Nord de France, F-59000 Lille, France
[c] CNRS UMR8181, Unité de Catalyse et Chimie du Solide, UCCS, F-59655 Villeneuve d'Ascq, France
[d] Ecole Nationale Supérieure de Chimie de Lille, ENSCL, F-59652 Villeneuve d'Ascq, France
[e] Institut Universitaire de France, Maison des Universités, 10 Boulevard Saint-Michel, 75005 Paris, France

ARTICLE INFO

Article history:
Received 1 December 2010
Revised 25 January 2011
Accepted 26 January 2011
Available online 2 March 2011

Keywords:
Rhenium and tantalum alkoxides
Catalysts
Methanol Conversion
DMM

ABSTRACT

Novel rhenium oxide catalysts have been prepared by impregnation of mesoporous TiO_2-anatase support using amounts of homometallic, such as $Re_4O_4(OEt)_{12}$, and heterometallic, such as $Ta_4O_2(OEt)_{14}(ReO_4)_2$, rhenium alkoxide solutions with subsequent thermal treatment. The structure of the produced catalytic centers was investigated by X-ray diffraction, XPS, and IR spectroscopy in order to examine the role of Re in enhancing catalytic activity. It has been demonstrated that rhenium is mostly present as perrhenate ligands attached via an oxo-bridge to an oxide surface. The catalytic activity was studied for the selective oxidation of methanol as model reaction, revealing selectivity strongly dependent on the nature of the molecular precursor: in case of ReO_x/TiO_2, the catalysts are showing selectivity to formaldehyde, and in case of $ReO_x/Ta_2O_5/TiO_2$ to DMM in rich conditions.

1. Introduction

The unique properties of rhenium oxide catalysts due to a variety of acidic and redox properties make them suitable materials for different types of catalytic reactions. For instance, Re_2O_7 has shown high catalytic activity in olefin metathesis and is the only catalyst that can work efficiently at room temperature [1]. Moreover, this heterogeneous catalyst can also be used to treat oleate esters when activated by organic derivatives of tin. However, their use is detrimental to the regeneration process [2]. Compared to Re_2O_7 on common γ-Al_2O_3, Re_2O_7 dispersed on α-Al_2O_3 has shown higher catalytic activity in the metathesis of internal as well as terminal olefins in the liquid phase [3,4]. Rhenium oxide supported on ordered mesoporous alumina has even been claimed as a more active and selective catalyst than Re_2O_7/γ-Al_2O_3 for alkene metathesis [5].

Nevertheless, even if this family of catalysts is quite active, they generally have a problem of application in catalytic selective oxidation reactions due to Re oxide sublimation under reaction conditions [6]. However, it was discovered that the rhenium oxide/zeolite catalyst was very active in the selective oxidation of benzene to phenol [7]. The most efficient catalyst based on Re is the well-known methyltrioxorhenium (CH_3ReO_3, MTO). This catalyst is particularly useful in oxidation chemistry and shows high activity for epoxidations, C—H and Si—H oxidations, and can also be applied in other types of catalytic reactions such as olefin metathesis and aldehyde olefinations [8–12].

Recently, it was shown that ReO_x-containing catalysts provide high catalytic activity and selectivity on a number of supports in certain conditions for partial oxidation of methanol to methylal (DMM) [13–16]. Numerous studies have shown that methanol oxidation is very sensitive to the nature of active sites and can be used to study the acidic and oxidation properties of catalytic surfaces [17–19]. The process of methanol oxidation leads to stepwise formation of formaldehyde (F), formic acid (FA), and finally CO_2. If the catalyst also has acidic properties, then the aforementioned products can react through a dehydration/condensation reaction with methanol to produce dimethylether (DME), dimethoxymethane (DMM), and finally methylformate (MF) (see Fig. 1).

Different properties of catalysts make therefore the methanol oxidation reaction also suitable as a surface probe, as proposed by [19], for the characterization of structural (crystallographic plane reactivity) and chemical (acid–base and redox) properties of oxide catalysts. The most interesting product for industry is DMM, which possesses a high degree of chemical stability while the absence of carbon–carbon bonds makes this compound a good candidate as a fuel additive. Industrially, methylal is produced by two-stage

* Corresponding author.
E-mail addresses: olesya.nikonova@kemi.slu.se (O.A. Nikonova), gulaim.seisenbaeva@kemi.slu.se (G.A. Seisenbaeva).

0021-9517/$ - see front matter © 2011 Elsevier Inc. All rights reserved.
doi:10.1016/j.jcat.2011.01.028

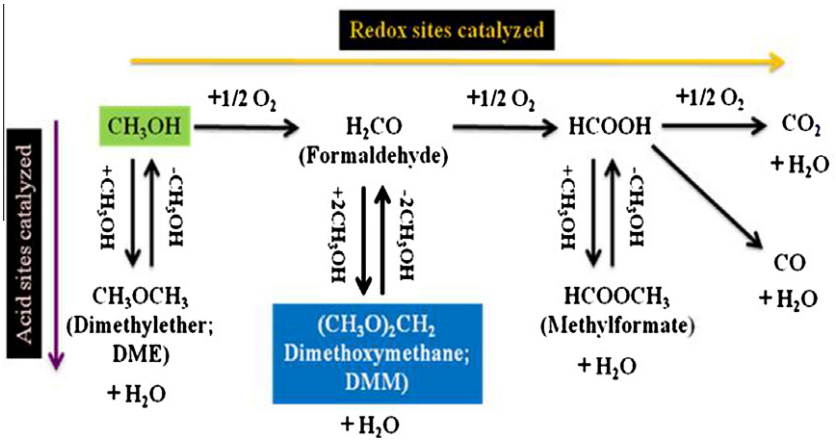

Fig. 1. Scheme of oxidation/dehydration of methanol.

processes: methanol oxidation to formaldehyde on silver and ferric molybdate catalysts and dehydrative condensation of the formaldehyde with methanol catalyzed by sulfuric acid. Thus, DMM production patents are rather scarce because of the difficulty of obtaining a high yield in DMM in one step. Different catalytic systems have been studied in oxidation of methanol into DMM such as VO_x—TiO_2 [20], $V_2O5 - TiO_2/SO_4^{2-}$ [21], Mo-supported catalysts [22] and FeMo-based catalysts [23,24]. Among these catalysts, it has been shown that ReO_x-based catalysts provide high activity and selectivity toward DMM in certain conditions [13,25] e.g. low conversion of methanol. It should be noted that these catalysts have the disadvantage of difficult preparation and poor stability under catalytic reaction.

In this work, we report the application of Re homo- and heterometallic alkoxide complexes as a new approach for the preparation of Re oxide-based catalysts. The catalysts have been prepared in one step at room temperature with subsequent calcination at 300 °C in air, resulting in the formation of crystalline phases based on Re, mainly in the oxidation state + VII, as monometallic oxide product and as a new bimetallic one based on Ta and Re. The latter bimetallic catalysts show an increased activity and selectivity in directing oxidation of methanol to DMM due to a synergetic effect between the rhenium oxide centers and the tantalum oxide phase.

2. Experimental

2.1. Synthesis of precursors

$Re_4O_4(OEt)_{12}$ (I) has been obtained by the anodic dissolution of rhenium metal in ethanol in an electrochemical cell without subdivision into cathode and anode space, supplied with a reflux condenser and water-cooling, as described in [26].

$Ta_4O_2(OEt)_{14}(ReO_4)_2$ (II) was obtained by the interaction of $Ta_2(OEt)_{10}$ with Re_2O_7 in dry toluene as it has been described in [27,28].

$Ta_2(OEt)_{10}$ (III) (tantalum (V) ethoxide, 99+% *Alfa Aesar*) was used as a precursor for the preparation of the Ta_2O_5/TiO_2 catalyst to compare the catalytic activity with the Re catalysts.

2.2. Preparation of catalysts

2.2.1. Support

The TiO_2-anatase support (titanium (IV) oxide catalyst support, *Alfa Aesar*) was calcined before use at 250 °C overnight in air and then transferred to a dessicator to avoid any traces of humidity.

2.2.2. Catalysts

Preparation of catalysts was carried out in two steps: the former involving impregnation of the TiO_2 support with a calculated amount of alkoxide solutions and the latter with thermal treatment of the catalysts at 300 °C in air for 2 h with an initial heating rate of 5 °C/min. In both steps, we had, as we expected, some losses of the Re presumably as Re_2O_7, due to the volatility of this oxide, and also of the organic part of the alkoxide complexes.

To obtain 1 wt% (S1) and 2 wt% (S2) of ReO_3/TiO_2, the calculated volumes of $Re_4O_4(OEt)_{12}$ alkoxide solution (0.032 mmol and 0.064 mmol) were used to impregnate 2.97 g and 2.94 g of pretreated TiO_2 support, respectively, followed by stirring of the mixture until complete infusion of alkoxide solutions into TiO_2. The samples were then dried in vacuum and left overnight to dry in air at room temperature. The next step of preparation was calcination of catalysts at 300 °C in air for 2 h with an initial heating rate 5 °C/min. The mass losses were not significant and observed for S1 and S2 as 2 wt%.

The desired amount of $Ta_4O_2(OEt)_{14}(ReO_4)_2$ alkoxide solution (0.064 mmol and 0.641 mmol) was used accordingly to prepare 1 wt% (S3) and 10 wt% (S4) of $ReO_3/Ta_2O_5/TiO_2$ catalysts. The applied procedures of impregnation with alkoxide solutions (II) were the same as described earlier. After thermal treatment of catalysts, the weight losses were observed as 5 wt% for both samples.

To provide an experimental reference to the catalytic activity of S3 and S4 catalysts, a material with 7 wt% TaO_x/TiO_2 (S5) was synthesized using $Ta_2(OEt)_{10}$ as the starting material. The aforementioned techniques were used for the preparation of this catalyst (S5). The calculated amount of (III) 1.9 mmol was impregnated on 4.65 g of pretreated TiO_2. After the thermal treatment, the weight loss was about 4 wt%, which corresponds only with the release of the organic part of the precursor (III).

2.3. Catalytic activity

Catalytic activity measurements were made using a fixed bed reactor described elsewhere [29]. Two different conditions in terms of methanol concentration were studied applying 7% methanol (poor condition) and 40% methanol (rich condition) diluted by air. After having passed through the catalytic bed, the reaction products were analyzed by online μ-gas chromatography (SRA) equipped with Poraplot U and 5 Å molecular sieve columns and TCD detectors. All the lines carrying methanol or reaction products were warmed up to 80 °C by heating tapes (Horst) to avoid condensation.

Table 1
Results of EDX analysis of the catalysts.

Composition	Ti		Ta		Re	
Catalyst	wt.%	at.%	wt.%	at.%	wt.%	at.%
S1	99.01 ± 2.08	99.74 ± 2.09			0.99 ± 0.03	0.26 ± 0.01
S2	98.08 ± 2.05	99.51 ± 2.09			1.88 ± 0.05	0.49 ± 0.01
S3	61.51 ± 1.29	85.81 ± 1.80	34.99 ± 0.98	12.94 ± 0.36	3.47 ± 0.10	1.25 ± 0.04
S4	62.57 ± 1.31	86.25 ± 1.81	28.97 ± 0.81	10.80 ± 0.30	9.75 ± 0.27	2.94 ± 0.08
S5	85.99 ± 1.81	95.86 ± 2.01	14.01 ± 0.39	4.14 ± 0.12		

2.4. Catalysts characterization

The specific surface areas of the catalysts were measured on a Quanta chrom – Quanta sorb apparatus using the single-point BET method, for the experimental details see Appendix Table A1.

Solid state FT-IR measurements in KBr pellets were recorded with a Perkin Elmer FT-IR spectrometer Spectrum-100. To establish the exact peak positions, the fitting of the peaks was carried out using Origin software.

SEM micrographs of the samples were obtained using a HITACHI TM-1000 scanning electron microscope equipped with an Oxford Instruments EDX detector. To obtain reliable statistics in the analysis, the data for each point were taken as average of 10 single measurements. The mapping across the analyzed surface was made by moving over the sample with steps of 8 μm.

The X-ray powder data collection was carried out at room temperature using a Bruker APEX II diffractometer (Mo Kα radiation, graphite-monochromator).

HRTEM investigations were performed on a JEOL JEM-2100F transmission electron microscope.

The XPS analyses were performed using a Kratos Analytical AXIS Ultra^{DLD} spectrometer. A monochromated aluminum source (Al Kα = 1486.6 eV) was used for excitation. The X-ray beam diameter was approximately 1 mm. The analyzer was operated at constant pass energy of 40 eV using an analysis area of approximately 700 μm × 300 μm. Charge compensation was applied to compensate for the charging effects that occurred during the analysis. The C 1s (285.0 eV) binding energy (BE) was used as internal reference. The spectrometer BE scale was initially calibrated against the Ag $3d_{5/2}$ (368.2 eV) level. Pressure was in the 10^{-10} torr range during the experiments. Simulation of the experimental photo peaks was carried out using CasaXPS software. Quantification took into account a nonlinear Shirley [30] background subtraction. The decomposition of the doublet Re $4f_{7/2}$—Re $4f_{5/2}$ was performed considering a spin–orbit splitting of 2.4 eV.

3. Results

3.1. SEM

After thermal treatment, all catalyst samples were investigated by SEM. To confirm the composition of all samples, the EDX analysis was performed on different parts of the catalysts/TiO_2 cylinders. First, the surfaces of the cylinders were investigated (see Table 1). The results corresponded in average to expected contents except for S5, where a higher content of Ta compared to the calculated one was detected on the surface.

To be able to understand this phenomenon, a crossover cut of catalysts/TiO_2 cylinders was made followed up by EDX analysis (see Fig. 2). In case of S1 and its analog S2, it was found that the ReO_x species were not uniformly distributed in the volume of TiO_2 cylinders. However, in the case of S3 and S4, better homogeneity was observed in the distribution of $TaReO_x$ species in the whole volume of the TiO_2 cylinders, while in the case of S5, the

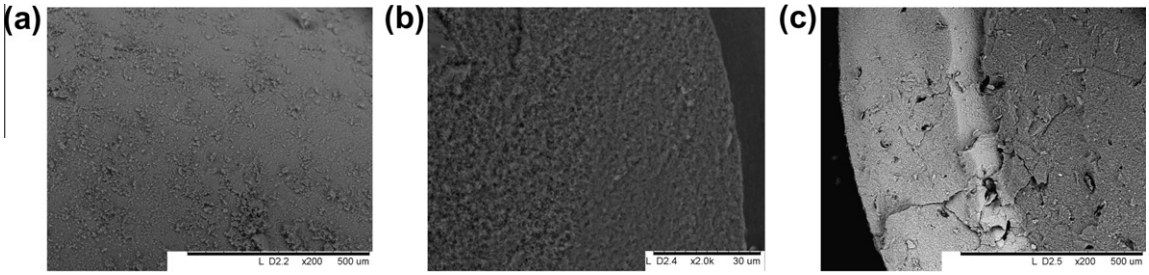

Fig. 2. SEM images: (a) surface of the S2; (b) crossover cut of S4 and (c) crossover cut of S5.

Table 2
IR spectra of catalysts (comparison with precursors $Re_4O_4(OEt)_{12}$ (**I**) and $Ta_4O_2(OEt)_{14}(ReO_4)_2$ (**II**)).

Vibrations (cm^{-1})	S1	S2	S3	S4	S5	(I)	(II)
δ(Re—O—Ti)	855 w br	832 s br					
ν(Re—O—Re)	874 w br	870 m br				878 w br	
ν(Re=O) (asymmetric stretching of $[ReO_4]^-$)	910 m 922 s br	911 m br	920 s	921 s		908 s 934 m	911 m 936 s 1021 m
ν(Ta—O—Re)			737 w br	860 m br			806 s 876 m 891 w
ν(Ta—O—Ti)					857 s br		
ν(Ta—O—Ta)			589 w br 610 m 666 s br	608 w br 652 m br	645 s br		478 w 521 m 563 m
ν(Ta—O)					949 w		

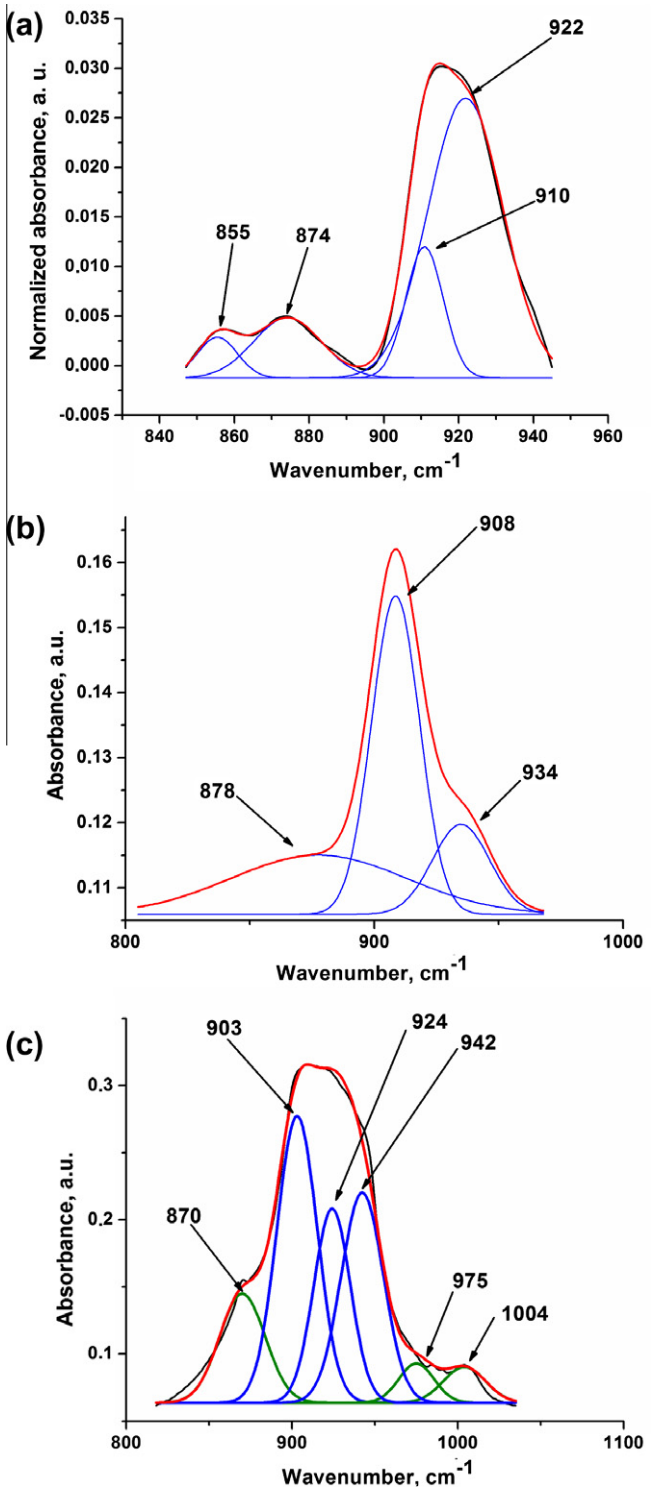

Fig. 3. IR spectra of (a) S1, (b) $Re_4O_4(OEt)_{12}$ (I), (c) mixture of Re_2O_7 and $HReO_4$.

TaO_x species were deposited closely to the surface with an impregnation depth of about 300 μm (see Fig. 2c – bright area due to heavy element contrast).

The observed difference in the deposition of the material can be explained in view of the different reactivity of the alkoxide precursors in relation to crystallization and hydrolysis/polycondensation.

The rhenium (V) ethoxide (I) cluster is known to be easily crystallized with higher crystal growth rate compared to that of nucleation. When $Re_4O_4(OEt)_{12}$ is crystallized, it is sensitive to oxidation, but stable to hydrolysis [26]. The islands of rhenium-rich materials apparently result from the thermal decomposition of the initially formed crystals.

The tantalum–rhenium ethoxide (II) is highly soluble and easily forms glass-like solids on drying, which explains uniform coating [27,28]. It should also be mentioned that we did not have any significant rhenium loss during preparation for the catalyst S4 according to the EDS analysis. The tantalum ethoxide (III) is known to be sensitive not only to hydrolysis, but also to ether elimination [31,32], easily forming dense oxide coatings [33]. The latter hinders the deeper diffusion of this precursor.

3.2. FT-IR

IR spectroscopy was used to determine the chemical groups present in the catalyst. Since TiO_2 has in the IR spectra a big broad band between 400 cm^{-1} and 880 cm^{-1}, all spectra were normalized and the TiO_2 phase signal was subtracted to reveal the peaks corresponding to loaded catalysts. After the fitting procedure, the positions of the peaks corresponding to different Re—O and Ta—O vibrations were identified (see Table 2).

To be able to distinguish differences between Re_2O_7 and ReO_4^- bands, the spectrum of the crystalline rhenium heptoxide (Sigma–Aldrich, rhenium (VII) oxide, ⩾99.9% metals basis), partially hydrolyzed to perrhenic acid during the preparation of the sample, was recorded (see Fig. 3c). The bands at 870 cm^{-1}, 975 cm^{-1}, and 1004 cm^{-1} could be assigned to Re_2O_7 according to [34], while the bands at 903 cm^{-1}, 924 cm^{-1}, and 942 cm^{-1} belong to ReO_4^- group in compliance with [35].

In case of S1 and S2, the vibrations at 855 cm^{-1} and 832 cm^{-1}, respectively, are close to the Re—O—H stretching modes reported in [35]. Since the samples of the catalysts did not contain OH-bonds or perrhenic acid, those peaks could be assigned to the Re-O—Ti vibrations. Peaks at 870 cm^{-1} and 874 cm^{-1} for samples S2 and S1, respectively, should be attributed to the Re—O—Re stretching mode, which is in good correlation with the peak at 878 cm^{-1} observed for the starting material $Re_4O_4(OEt)_{12}$ (I) and at 870 cm^{-1} for Re_2O_7 (see Fig. 3).

The Re=O stretching modes for the $Re_4O_4(OEt)_{12}$ alkoxide complex are considerably different from those for S1 as well as S2, where the vibrations at 910 cm^{-1}, 922 cm^{-1}, and 911 cm^{-1} could be assigned to vibrations of the perrhenate group $[ReO_4]^-$ according to [35] (see Fig. 3). The samples S1 and S2 contain a mixture of two different species, Re_2O_5 and ReO_4^-, according to the IR spectra (see Fig. 3) and XPS results, which can be explained by the properties of the $Re_4O_4(OEt)_{12}$ complex. The alkoxide precursor (I) contains rhenium in the oxidation state + V. On its thermal decomposition, it is then partially oxidized into Re (VI–VII).

For the catalyst S5, three peaks have been detected corresponding to different types of vibrations: the first one at 645 cm^{-1} to Ta—O—Ta and two others to Ta—O, while the peaks observed for the precursor $Ta_4O_2(OEt)_{14}(ReO_4)_2$ (II) are situated at the range 478–563 cm^{-1} (see Fig. 4). It should be mentioned that the appearance of the peak at 949 cm^{-1} indicates the presence of suboxides [36]. Almost the same position of peaks of the Ta—O—Ta vibrations can be found for S3 and S4 (see Fig. 4c and d). As expected, the vibrations for Ta—O—Re stretching modes could be observed at 737 cm^{-1} and 860 cm^{-1} for S3 and S4, respectively, which are in good correlation with bands for the staring material $Ta_4O_2(OEt)_{14}(ReO_4)_2$ (II) (see Fig. 4b). It should be noted that while for S1 and S2, both Re—O—Re and Re=O vibrations were detected, for S3 and S4 only the last one at 920 cm^{-1} was observed, at the same position as for the starting material, which can be explained by the preservation of the perrhenate unit already present in the precursor $Ta_4O_2(OEt)_{14}(ReO_4)_2$.

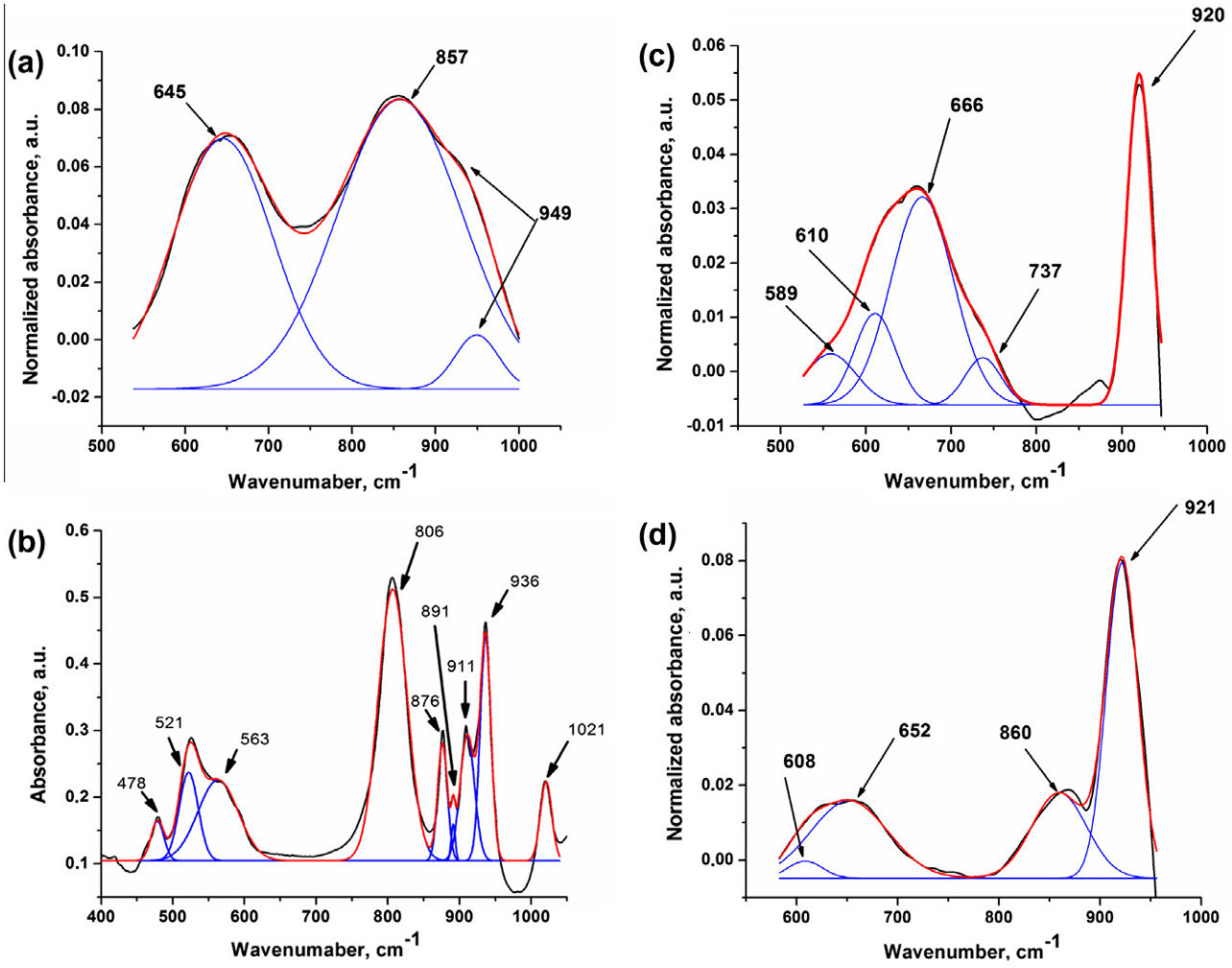

Fig. 4. IR spectra of (a) S5, (b) $Ta_4O_2(OEt)_{14}(ReO_4)_2$ (II), (c) S3, (d) S4.

Table 3
Results of XPS analysis (unit: at.%).

	S1	S2	S3	S4	S5
Re	0.2	0.1	2.7	8.6	
Ti	99.8	99.9	91.6	62.2	85.6
Ta			5.7	29.2	14.4

3.3. XPS

In order to confirm the aforementioned hypothesis, the outer atomic layers up to 50 Å were scanned using X-ray photoelectron spectroscopy. Table 3 presents the results obtained for the series.

XPS analysis exhibits almost the same composition for samples S1 and S2. The results obtained by XPS and EDS analysis showed a significant difference in content of the surface of the crystallites and the bulk samples. It could be confirmed that the external 50 Å of the TiO_2 crystallites were poorer in rhenium than the volume studied by EDS. The XPS spectra show that the rhenium atoms are present in oxidation state + V or +VI for outer shells of these two samples. The principal Re $4f_{7/2}$ component, located at 44.1 eV for S1 and 43.7 eV for S2 respectively, could be referred to Re_2O_5 or ReO_3 according to [37]. The slight shift could be explained by the lower content of Re in the S2 sample. The peak positions for the Ti 2p and O 1s were at 458.8 and 530.1 eV, respectively.

The sample S5 showed an important quantity of 14 at.% tantalum at the surface. As expected, the BE corresponding to Ta $4d_{5/2}$ exhibited typically at 230.6 eV corresponding to Ta atoms in the oxidation state + V [[38] and Ref. therein].

Concerning two other samples S3 and S4, it seems that the catalysts have the $TaReO_x$ phases at the surface with Ta/Re ratios equal to 3.3 and 2.1, respectively. The thickness of the $TaReO_x$ layer increased as a higher quantity of each element (i.e. Ta and Re) was observed, correlating with the decrease in the Ti content analyzed by XPS (see Table 3). This indicates a better dispersion of the active phase on the surface of the TiO_2 support ((Re + Ta)/Ti = 0.6 and 0.1 for S4 and S3, respectively). The oxidation state of Re in these two samples is mainly + VII with a binding energy of the Re $4f_{7/2}$ equal to 46.3 eV corresponding to ReO_4^- [37], a minor contribution of Re + VI is clearly evidenced for the sample S3 by a peak at 44.4 eV corresponding to ReO_3. To prove the presence of Re + VI is not straightforward on the S4 sample. The Ti 2p and O 1s photopeaks occurred in the typical areas for TiO_2 at 459.0 eV and 530.2 eV, respectively.

3.4. XPD and HRTEM

All samples were represented mainly by anatase form of TiO_2 in the X-ray powder patterns. Only some extra peaks identified in Fig. 5 could be referred to catalytic phases in the samples (see Fig. 5).

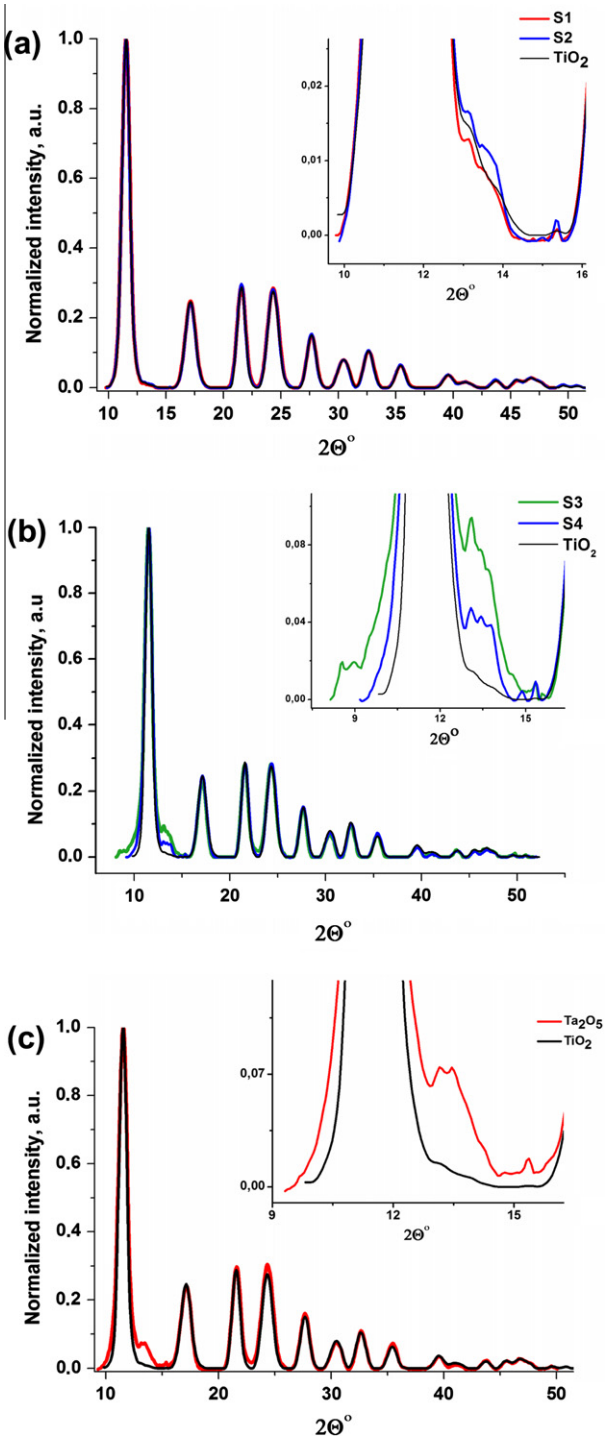

Fig. 5. Results of XPD of (a) S1 and S2, (b) S3 and S4, (c) S5.

Furthermore, the XPD results have indicated that the grain size of crystallites of the catalysts decreased with the loading of catalysts onto the support. From the TEM images, it can be seen that particles are present as agglomerates. Fig. 6 displays representative TEM images for S1 and S4 samples. The SAED image analysis shows polycrystallinity of the samples, which made it difficult to determine the structure of the catalyst phase (see Fig. 6).

3.5. Catalytic activity

The methanol oxidation reaction on all the catalysts was performed at 275 °C under poor and rich conditions with 7% and 40% of methanol, respectively, diluted by air with an approximate flow of 40 ml/min. It was found that the conversions increased with the reaction temperature for each sample. Table 4 shows the catalytic results for all catalysts at the higher and lower methanol conversion. In each case, the quantity of oxygen was enough and there were no limitations in performing oxidation reaction caused by low oxygen concentration.

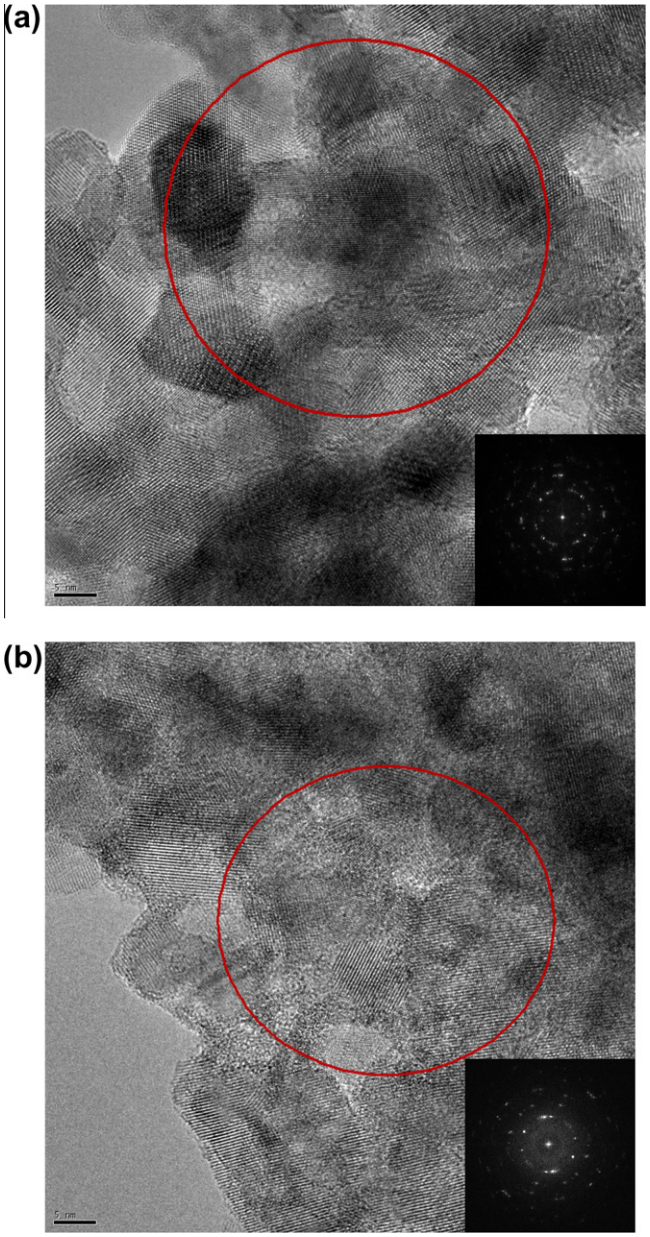

Fig. 6. HRTEM images of S1 and S4 samples.

It could be seen that the activities for the two samples, S1 and S2, were comparable revealing methanol conversion of 14% and 11% in the poor condition and 6.5% and 4% in the rich condition, respectively. In this case, the selectivity for both catalysts was mainly toward F at rich conditions (see Table 4). It should also be noted that the CO_x molecules were present in a non-negligible quantity especially in the poor methanol condition (see Table 4). On the contrary, when the quantity of methanol (rich condition) was increased, these molecules almost disappeared (see Fig. 7).

For S3 and S4 samples, the main product at each temperature was DMM (see Fig. 8) in rich condition. It is worth noting that the

Table 4
Catalytic results.

Sample	MeOH vol (%)	Max MeOH conversion in (%)	MeOH conversion (mol)	S(F)	S(FM)	S(DME)	S(DMM)	S(CO)	S(CO_2)
TiO_2	7	6	0.42	41	17	42			
	40	4	1.6	49		44	7		
S1	7	14	0.98	41	17	28		13	1
	40	6.5	2.6	43	11	26	20		
S2	7	11	0.77	39	15	30		15	1
	40	4	1.6	37	13	30	17	2	1
S3	7	37	2.59	40	17	15		26	2
	40	15	6	15	17	12	52	3	1
S4	7	43	3.01	39	19	15	1	21	5
	40	23	9.2	6	13	11	67	1	1

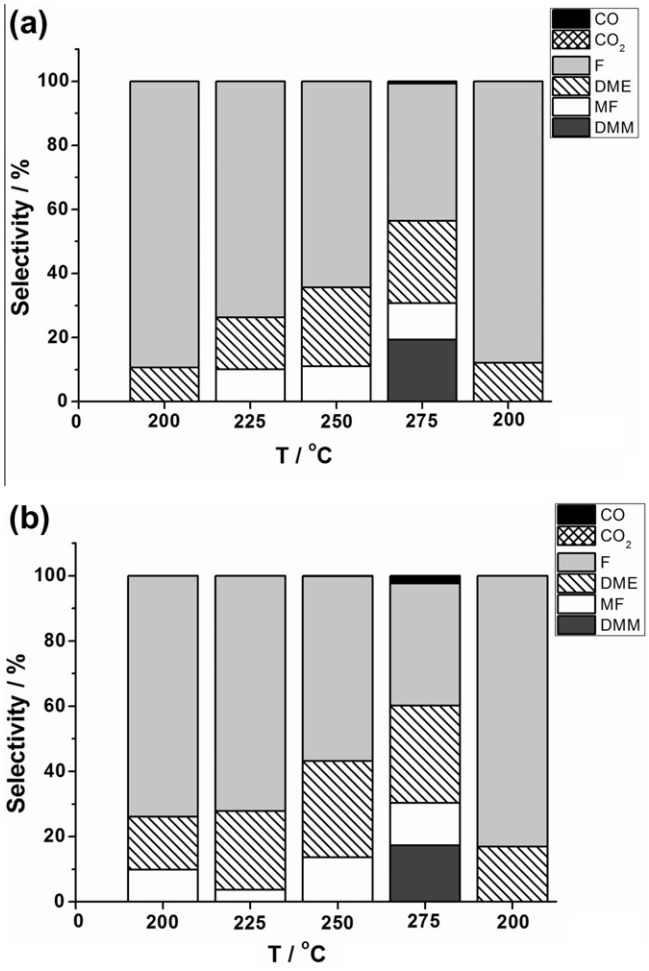

Fig. 7. Selectivity of S1 (a) and S2 (b) function of temperature in rich methanol condition.

selectivity increased with temperature up to 250 °C and then decreased. In order to verify the catalyst survival at the end of the experiment, the decrease in the temperature to 200 °C demonstrated an increase in DMM selectivity. The other detected products were MF, DME, and F, with almost no trace of CO_x as evidenced in rich condition, while the opposite tendency was observed in poor condition (see Table 4). It should also be noted that in case of 7% methanol conversions, the selectivity of S3 and S4 was mainly toward formaldehyde and no DMM formation occurred.

This knowledge permitted to evaluate the redox and acidic properties of S3 and S4. To be able to understand different properties of ReO_x/TiO_2 and $ReTaO_x/TiO_2$ catalysts, a Ta_2O_5/TiO_2 catalyst was obtained. The Ta atoms in S5 effectively add acidic property to the support (main product is DME) without changing drastically the methanol conversion, which did not exceed 6% in rich methanol condition (see Fig. 8c).

4. Discussion

SEM investigation demonstrated that the distribution of the catalysts occurred in different ways. In fact, for S1 and S2, the distribution of the precursor of ReO_x species, the $Re_4O_4(OEt)_{12}$ alkoxide, resulted in a difficulty in spreading them evenly in the whole volume of TiO_2 cylinders. On impregnation of TiO_2 cylinders, the specific behavior of the precursor caused, in case of S5, the formation of a dense TaO_x layer with a thickness of about 300 μm. However, in the case of S3 and S4, another trend resulting in better distribution through the volume of TiO_2 cylinders was observed. These phenomena could be explained by the nature and properties of the starting materials as described earlier.

The BET results did not show significant increases in the specific surface areas of the catalysts (the average value for all samples was 15 m^2/g) in comparison with the support (14 m^2/g), but at the same time, it did not decrease the observable surface area for the TiO_2. This can be explained by the formation of a relatively thin layer of catalysts on the surface of the substrate hindering closing or filling of the original mesopores, but not creating considerable volumes of an additional porous phase.

The FT-IR results demonstrated that all samples contained the perrhenate group $[ReO_4]^-$. According to IR spectra investigations, the catalytic $O_3Re{-}O$ group was connected to the TiO_2 support through the oxo-bridge in the case of S1 and S2 samples. In the case of S3 and S4, the perrhenate group was connected through oxo-bridges to Ta atoms. Since in the Ta_2O_5/TiO_2 catalyst, the Ta atoms were connected to the support through oxo-bridges, it is plausible to suggest that in the catalysts S3 and S4, the same type of connection is present. This would mean that the ReO_x species were in turn situated on the surface of the coating, which would explain the selectivity of these catalysts toward DMM caused by the presence of more acidic TaO_x species compared to the TiO_2 [39].

According to XPS data for S1 and S2, the Re atoms were present mainly in the oxidation state + V or +VI, while for S3 and S4 samples, they were in the oxidation state + VII. Moreover, it should be mentioned that ReO_x species were reduced onto the surface of the support. These phenomena resulted in the appearance of extra peaks corresponding to rhenium in oxidation state + VI in the S3 sample. Thus, the reduced rhenium oxide species help in keeping a good activity and selectivity of our catalysts.

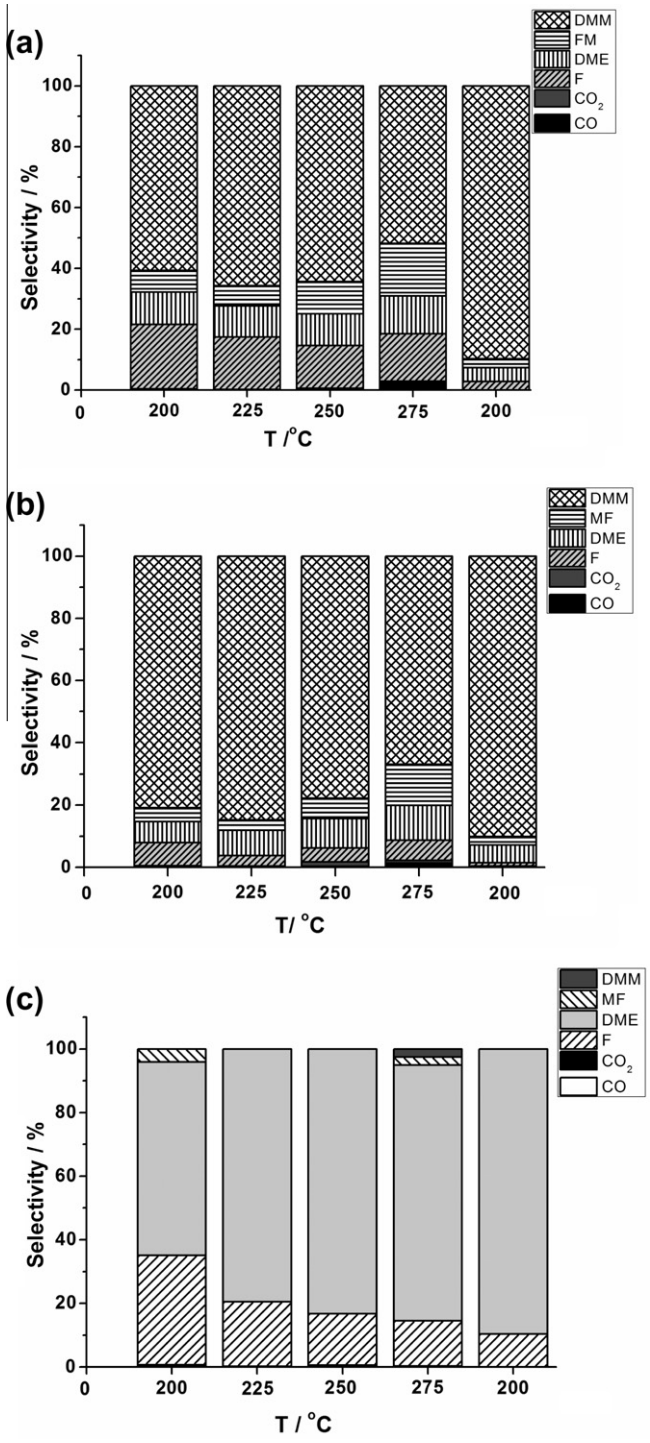

Fig. 8. Selectivity of S3 (a), S4 (b), and S5 (c) function of temperature in rich methanol condition.

In terms of selectivity, the Re oxide species supported on TiO_2 supports (S1 and S2) appeared to have a good balance between redox and acidic properties in order to form DMM and MF, which were not present at all or were formed in very small quantities for the TiO_2 support alone. According to Table 4, the methanol conversion decreased with the rhenium loading in poor and rich methanol conditions for S3 and S4. In terms of selectivity, in the poor methanol condition, the main product was formaldehyde (SF ~40%), meaning that the redox properties were dominant under this condition or that the adsorption energy was lower than the one needed to process to the dehydration/condensation reaction producing DMM. Nevertheless, the presence of MF seems to be proof that the redox/acidic properties were revealed simultaneously in these catalysts. Increase in the quantity of methanol in the feed, resulting in the increase in probability of higher methanol adsorption on the surface of the catalysts, favors condensation of formaldehyde with methanol producing DMM. Table 4 shows that DMM selectivity reaches more than 50% for both S3 and S4 samples. At the same time, the selectivity toward F decreases drastically, which seems to be in agreement with our previous assumptions. The mixed oxidation numbers + VI and +VII for rhenium in the S3 and S4 samples increased drastically the DMM selectivity under rich methanol condition. It seems that the assumption claimed by Iwasawa et al. [15] is true but not sufficient. The fact that the two oxidation states are present in the catalysts permits the formation of formaldehyde, but then the adsorption energy should be strong enough to keep the methoxy group at the surface of the catalyst during its reaction with two methanol molecules, which leads to the formation of DMM.

5. Conclusions

The application of alkoxide molecular precursors permits the creation of new rhenium and chemically connected rhenium–tantalum catalysts on mesoporous TiO_2 supports. The materials were obtained in ambient atmosphere with subsequent calcination at a relatively low temperature of 300 °C for 2 h leading to crystalline products. The results of FT-IR and XPS investigations showed that Re is present mainly in the oxidation state + VII as a perrhenate group for samples S3 and S4. The reduced rhenium oxide sites of the samples help to keep the activity during and at the end of the catalytic reaction of the produced catalysts. The small values of the BET surface areas do not influence the catalytic properties of the samples. The selectivity of samples S1 and S2 was mostly toward formaldehyde, but in the case of S3 and S4, the product of the methanol oxidation was DMM. The simultaneous presence of the chemically connected oxidative (perrhenate) and acidic (tantalum oxide) components in the catalyst apparently permit one-step production of DMM.

Acknowledgments

The authors express their gratitude to Prof. Vadim Kessler for fruitful discussions. We are very grateful to the Faculty of Natural Resources SLU for the support in purchasing the Hitachi TM-1000 scanning electron microscope. As well, we are grateful for possibilities to use TEM at Berzelii center EXSELENT on Porous Materials at Department of Materials and Environmental Chemistry at Stockholm University. Authors want to thank M. Sundberg, C.-W. Tai, A. Beaurain, M. Trentesaux, and G. Tesquet for their technical help.

Appendix A. Supplementary material

Supplementary data associated with this article can be found, in the online version, at doi:10.1016/j.jcat.2011.01.028.

References

[1] J.C. Mol, Catal. Today 51 (1999) 289.
[2] J.C. Mol, Top. Catal. 27 (2004) 97.
[3] P.C. Bakala, E. Briot, Y. Millot, J.-Y. Piquemal, J.-M. Bregeault, J. Catal. 258 (2008) 61.
[4] M. Onaka, T. Oikawa, Chem. Lett. 31 (2002) 850.
[5] T. Oikawa, T. Oosohi, T. Tanaka, T. Yamamoto, M. Onaka, Micropor. Mesopor. Mater. 74 (2004) 93.
[6] S. Albonetti, F. Cavani, F. Trifiro, Catal. Rev. Sci. Eng. 38 (1996) 413.
[7] T. Kusakari, T. Sasaki, Y. Iwasawa, Chem. Commun. (2004) 992.

[8] R. Buffon, A. Auroux, F. Lefebvre, M. Leconte, A. Choplin, J.-M.A. Basset, J. Mol. Catal. 76 (1992) 287.
[9] K.R. Jain, F.E. Kühn, J. Organom. Chem. 692 (2007) 5532.
[10] A. Salameh, A. Baudoin, S. Daravong, V. Boehm, M. Roeper, J.-M. Basset C. Coperet, J. Catal. 253 (2008) 180.
[11] A. Salameh, J. Joubert, A. Baudouin, W. Lukens, F. Delbecq, P. Sautet, J.M. Basset, C. Coperet, Angew. Chem. Int. Ed. 18 (2007) 3870.
[12] R. Buffon, A. Choplin, M. Leconte, J.-M. Basset, J. Mol. Catal. 72 (1992) L7.
[13] Y. Yuan, T. Shido, Y. Iwasawa, Chem. Commun. 15 (2000) 1421.
[14] A.S.Y. Chang, W. Chen, H. Wang, J.E. Rowe, T.E. Madey, J. Phys. Chem. B 108 (2004) 14643.
[15] Y. Yuan, H. Liu, H. Imoto, T. Shido, Y. Iwasawa, J. Catal. 195 (2000) 51.
[16] Y. Yuan, Y. Iwasawa, J. Phys. Chem. B 106 (2002) 4441.
[17] L.E. Briand, W.E. Farneth, I.E. Wachs, Catal. Today 62 (2000) 219.
[18] Y. Matsuoka, M. Nywa, Y. Murakami, J. Phys. Chem. 94 (1990) 1477.
[19] J.-M. Tatibouët, Appl. Catal. A: Gen. 148 (1997) 213.
[20] H. Guo, D. Li, D. Jiang, W. Li, Y. Su, Catal. Commun. 11 (2010) 396;
Y. Fu, J. Shen, Chem. Commun. 21 (2007) 2172;
J. Liu, Y. Fu, Q. Sun, J. Shen, Micropor. Mesopor. Mater. 116 (2008) 614;
J. Liu, Q. Sun, Y. Fu, J. Shen, J. Colloid Interface Sci. 335 (2009) 216.
[21] H. Zhao, S. Bennici, J. Shen, A. Auroux, J. Catal. 272 (2010) 176.
[22] M. Brandhorst, S. Cristol, M. Capron, C. Dujardin, H. Vezil, G. Lebourdon E. Payen, Catal. Today 113 (2006) 34;
M. Fournier, A. Aouissi, C. Rocchiccioli-Deltcheff, J. Chem. Soc. Chem. Commun. 3 (1994) 307;
C. Rocchiccioli-Deltcheff, A. Aouissi, M.M. Bettahar, S. Launay, M. Fournier, J. Catal. 164 (1996) 16;
C. Rocchiccioli-Deltcheff, A. Aouissi, S. Launay, M. Fournier, J. Mol. Catal. A: Chem. 114 (1–3) (1996) 331;
H. Liu, E. Iglesia, J. Phys. Chem. B 107 (39) (2003) 10840;
H. Liu, E. Iglesia, J. Catal. 223 (1) (2004) 161.
[23] J. Gornay, X. Secordel, M. Capron, G. Tesquet, P. Fongarland, E. Payen J.-L. Dubois, F. Dumeignil, Oil and Gas Sci. Tech. – Rev. IFP Energies Novellas 65 (2010) 751.
[24] J. Gornay, X. Sécordel, B. de Ménorval, S. Cristol, P. Fongarland, M. Capron L. Duhamel, E. Payen, J.-L. Dubois, F. Dumeignil, Green Chem. 12 (2010) 1722.
[25] X. Secordel, E. Berrier, M. Capron, S. Cristol, J.-F. Paul, M. Fournier, E. Payen, Catal. Today 155 (2010) 177.
[26] O.A. Nikonova, K. Jansson, V.G. Kessler, M. Sundberg, A.I. Baranov A.V. Shevelkov, D.V. Drobot, G.A. Seisenbaeva, Inorg. Chem. 47 (2008) 1295.
[27] O.A. Nikonova, V.G. Kessler, D.V. Drobot, P.A. Shcheglov, G.A. Seisenbaeva, Polyhedron 26 (2007) 862.
[28] O.A. Nikonova, G.A. Seisenbaeva, V.G. Kessler, P.A. Shcheglov, D.V. Drobot, Russ. J. Inorg. Chem. 52 (2007) 1687.
[29] S. Royer, X. Sécordel, M. Brandhorst, F. Dumeignil, S. Cristol, C. Dujardin M. Capron, E. Payen, J.-L. Dubois, Chem. Commun. 7 (2007) 865.
[30] D.A. Shirley, Phys. Rev. B 5 (1972) 4709.
[31] D.C. Bradley, B.N. Chakravarti, W.J. Wardlaw, J. Chem. Soc. (1956) 4439.
[32] V.G. Kessler, N.Y. Turova, A.I. Yanovsky, A.I. Belokon', Y.T. Struchkov, Russ. J. Inorg. Chem. 36 (1991) 1662.
[33] P. Werndrup, M. Verdenelli, F. Chassagneux, S. Parola, V.G. Kessler, J. Mater. Chem. 14 (2004) 344.
[34] I.R. Beattie, T.R. Gilson, P.J. Jones, Inorg. Chem. 35 (1996) 1301.
[35] M.R. Mohammed, W.F. Sherman, J. Phys. C: Solid State Phys. 14 (1981) 4121.
[36] N. Dharmaraj, H.C. Park, C.H. Kim, P. Viswanathamurthi, H.Y. Kim, Mater. Res. Bull. 41 (2006) 612.
[37] A. Naor, N. Eliaz, L. Burstein, E. Gileadi, Electrochem. Solid-State Lett. 13 (2010) D91.
[38] S.F. Ho, S. Contarini, J.W. Rabalais, J. Phys. Chem. 91 (1987) 4779.
[39] Y. Chen, J.L.G. Fierro, T. Tanaka, I.E. Wachs, J. Phys. Chem. B 107 (2003) 5243.